PDF sensitivity studies from ATLAS measurements

Rémie Hanna – CEA/IRFU
On behalf of the ATLAS collaboration

QCD@LHC 2015
1-5 September 2015
Queen Mary, University of London

Irfu - CEA Saclay
Institut de recherche sur les lois fondamentales de l'Univers

ATLAS EXPERIMENT

PDF sensitivity studies from ATLAS measurements

Why do we need to constrain PDFs?

- Significant source of uncertainty on Higgs production*, large impact on the discovery reach of new massive particles, ...

		σ (8 TeV)	uncertainty *
NNLL QCD +NLO EW	gg→H	19.5 pb	14.7%
	VBF	1.56 pb	2.9%
NNLO QCD +NLO EW	WH	0.70 pb	3.9%
	ZH	0.39 pb	5.1%
NLO QCD	ttH	0.13 pb	14.4%

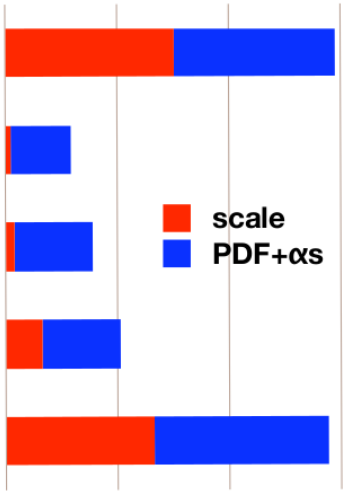

J. Campbell, ICHEP2012

- The ATLAS electroweak measurements affected by PDF uncertainties presented in this talk :
  - ✔ Weak mixing angle
  - ✔ W-mass

** With N³LO calculations, scale uncertainties decreased. Also, with the new round of PDFs, the differences between the different sets will get similar to N³LO scale uncertainties, but still be a significant source of uncertainty.*

PDF sensitivity studies from ATLAS measurements

How can ATLAS data constrain the PDFs?

- Inclusive W/Z cross-sections
- Low and High Mass Drell-Yan
- W+c production
- Jet and photon cross-sections
- Top quark production
- Z-transverse momentum

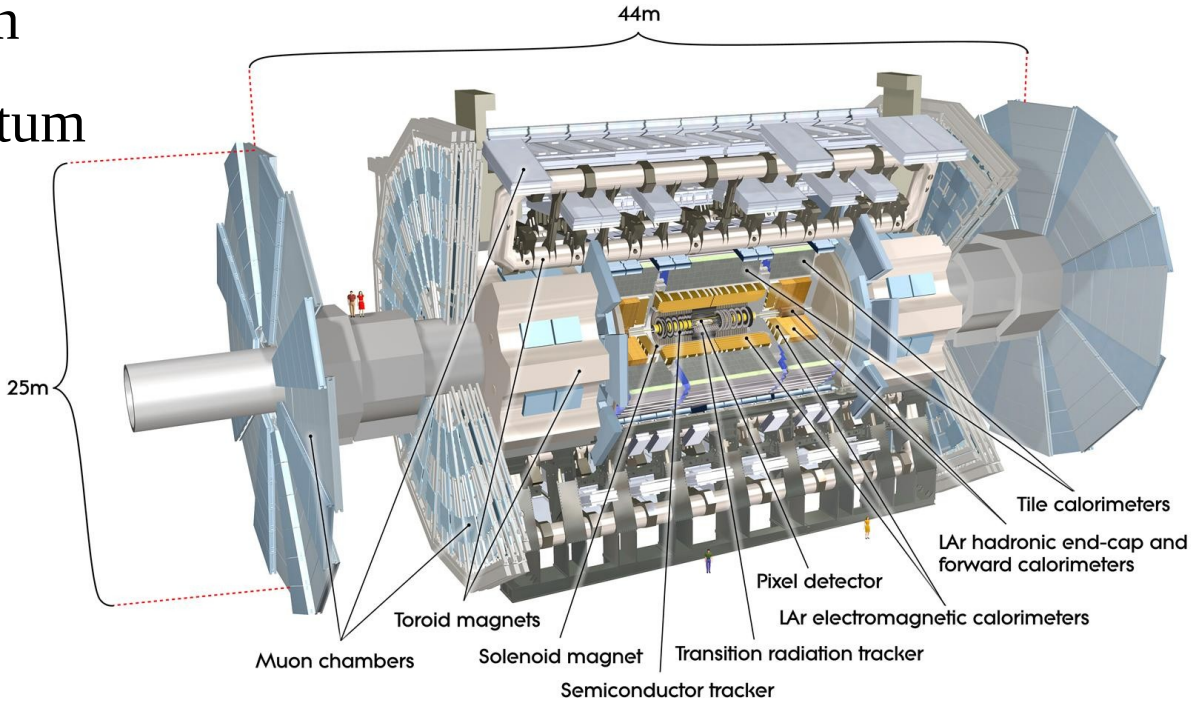

Part I

Precision Electroweak Measurements affected by PDF uncertainties

Precision electroweak measurements affected by PDF uncertainties

1) Weak mixing angle

arXiv:1503.03709, submitted to JHEP

A forward-backward asymmetry A_{FB} in the polar angle θ between the final state leptons and the incoming quark direction, is observed in $q\bar{q} \to Z/\gamma^* \to \ell^+\ell^-$ processes in the rest frame of the dilepton system (Collins-Soper frame)

$$\cos\theta^*_{CS} = \frac{p_{z,\ell\ell}}{|p_{z,\ell\ell}|} \frac{2(p_1^+ p_2^- - p_1^- p_2^+)}{m_{\ell\ell}\sqrt{m_{\ell\ell}^2 + p_{T,\ell\ell}^2}} \quad \text{where} \quad p_i^{\pm} = \frac{1}{\sqrt{2}}(E_i \pm p_{z,i})$$

The weak mixing angle can be extracted from the asymmetry $A_{FB} = \frac{\sigma_F - \sigma_B}{\sigma_F + \sigma_B}$

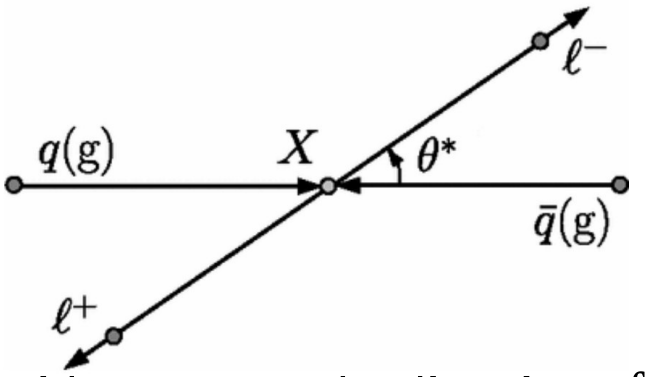

The sign of $\cos\theta^*_{CS}$ is defined with respect to the direction of the incoming quark, which is unknown in *pp* collisions.

Precision electroweak measurements affected by PDF uncertainties

1) Weak mixing angle

arXiv:1503.03709, submitted to JHEP

- The forward direction ($\cos\theta^*_{CS} \geq 0$) is defined as the direction of the longitudinal boost of the lepton pair.

- PDFs cause a dilution of the observed asymmetry and the associated uncertainties
- The results depend on the chosen PDF.
- The combined result (central and forward electrons, and muons) :

  $\sin^2\theta_{eff}$ = 0.2308 ± 0.0005(stat.) ± 0.0006(syst.) ± 0.0009(PDF) = 0.2308 ± 0.0012

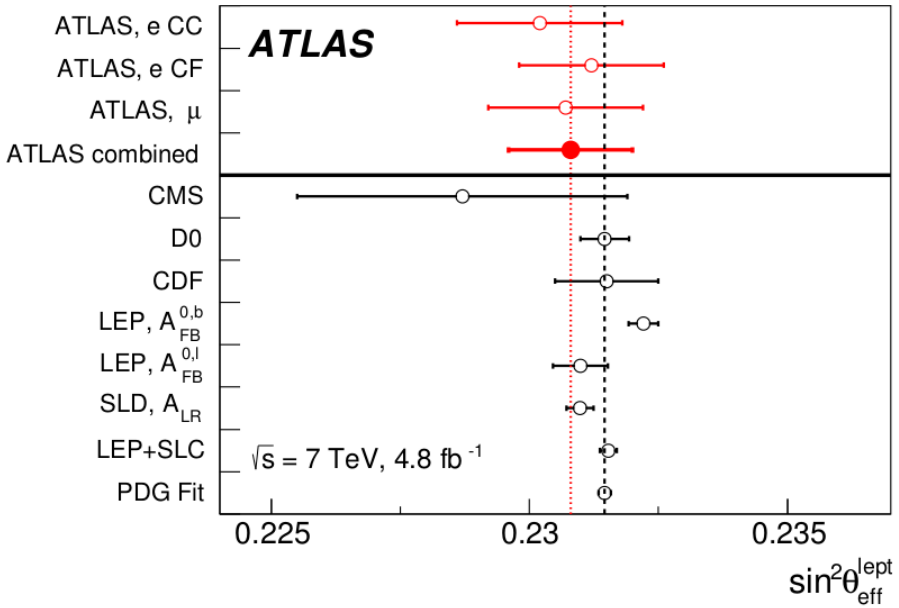

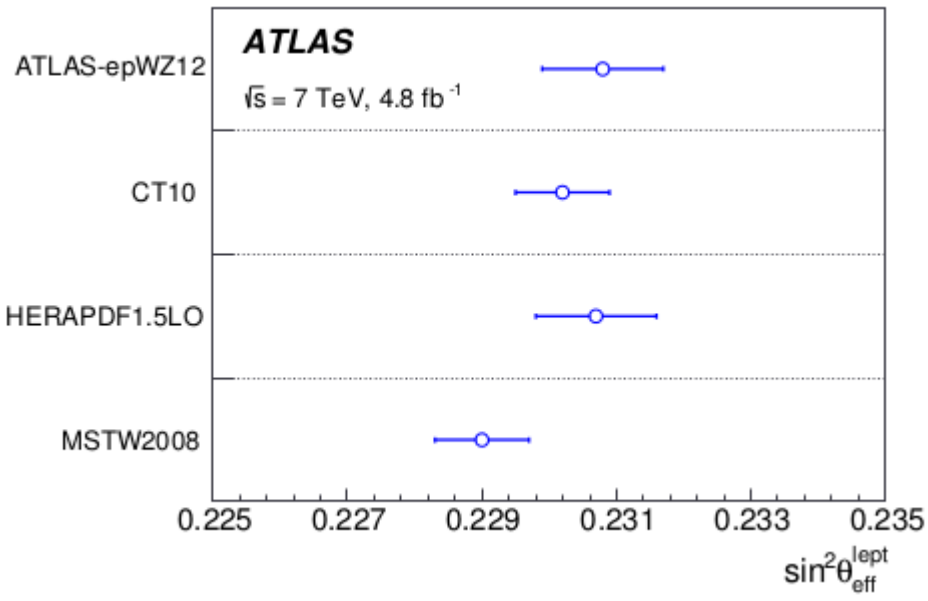

Precision electroweak measurements affected by PDF uncertainties

2) W-boson mass (existing results)

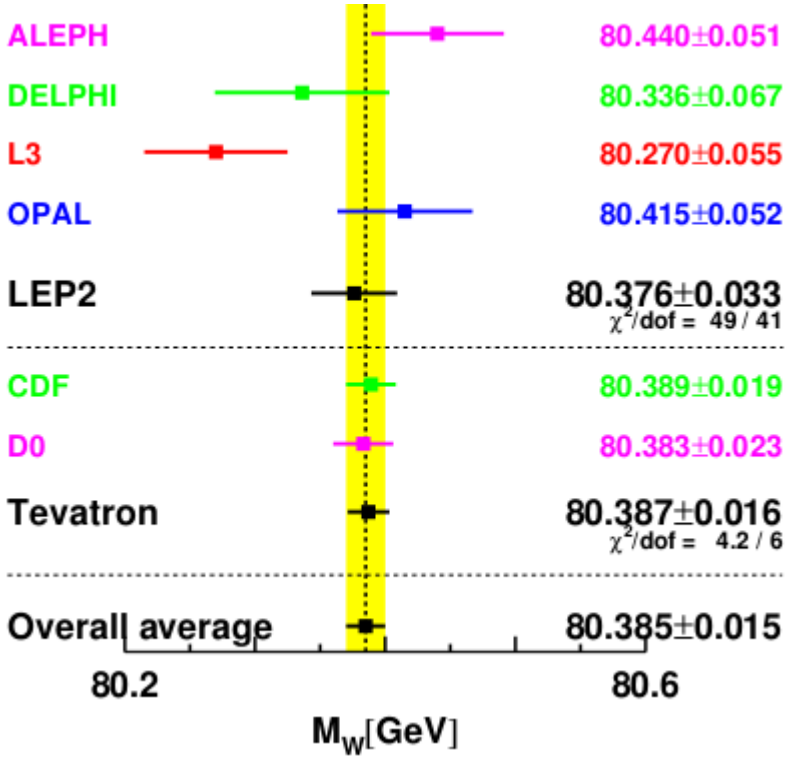

m_W is measured using the transverse mass ($m_T^2 = 2\, p_T^l\, p_T^\nu [1 - \cos\Delta\phi(l,\nu)]$) and the transverse lepton momentum (p_T^l) distributions.

The indirect (EW fit) determination of m_W (δm_W = 8 MeV - Eur.Phys.J.C74(2014)3046) is more accurate than the measured value (δm_W = 15 MeV) including the latest measurements of CDF and DØ → natural goal at the LHC would be $\delta m_W < 10$ MeV.

Precision electroweak measurements affected by PDF uncertainties

2) W-boson mass (PDF uncertainties)

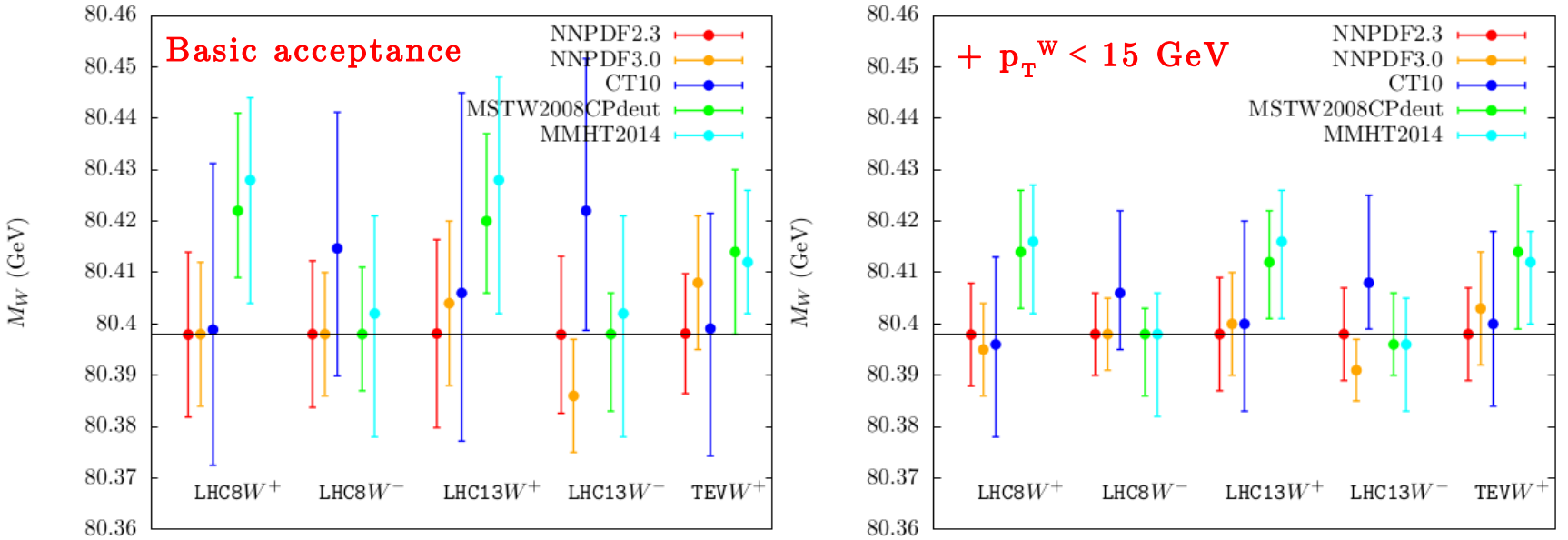

G. Bozzi, L. Citelli, A. Vicini - Phys. Rev. D 91, 113005 (2015)

- Lepton p_T only
- The p_T^W cut reduces large *x* contributions (at generator level)
- Each set can achieve 10 MeV by itself, but the spread of the central values is larger than the estimated uncertainty

- PDF uncertainties (and arising from low-p_T^W) were also investigated in an ATLAS study (ATL-PHYS-PUB-2014-015) in the context of a W-mass measurement.

Part II
Constraining the PDF

Strange quark density, strange-to-down sea quark distributions ratio

Constraining the PDF

1) Inclusive W/Z cross-sections

35 pb^{-1} of 7 TeV data (2010)

Phys.Rev.Lett. 109 (2012) 012001
– Phys. Rev. D85, 072004 (2012)

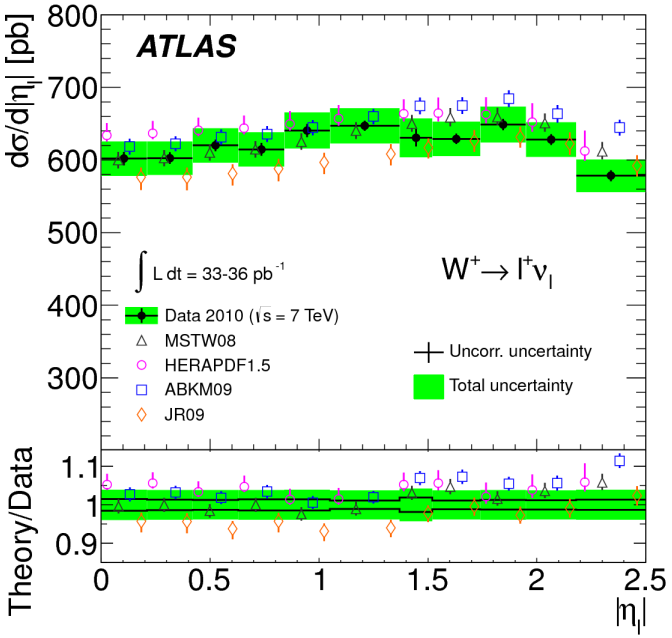

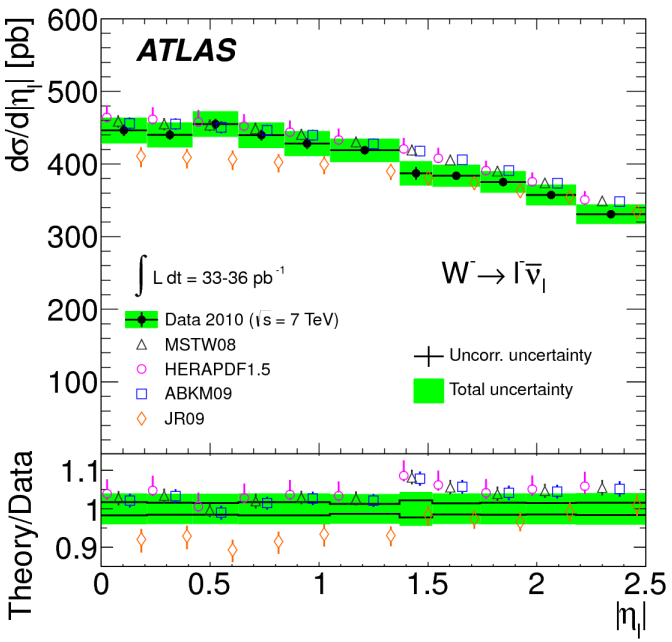

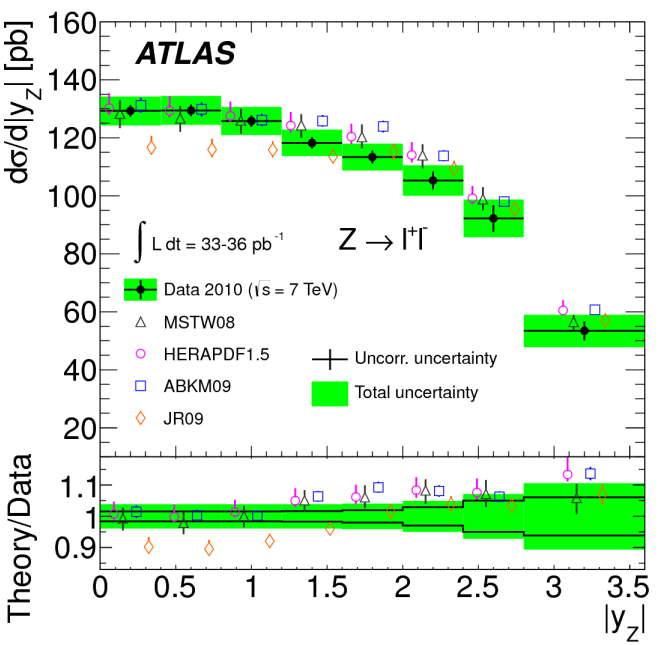

W± and Z cross section measurements are compared to NNLO predictions using different PDF sets. They are generally well described by the predictions, with a few deviations observed.

Strange quark density, strange-to-down sea quark distributions ratio

Constraining the PDF

1) Inclusive W/Z cross-sections

35 pb^{-1} of 7 TeV data (2010)

Phys.Rev.Lett. 109 (2012) 012001
– Phys. Rev. D85, 072004 (2012)

- NNLO fits using ATLAS data (epWZ) + DIS data from HERA

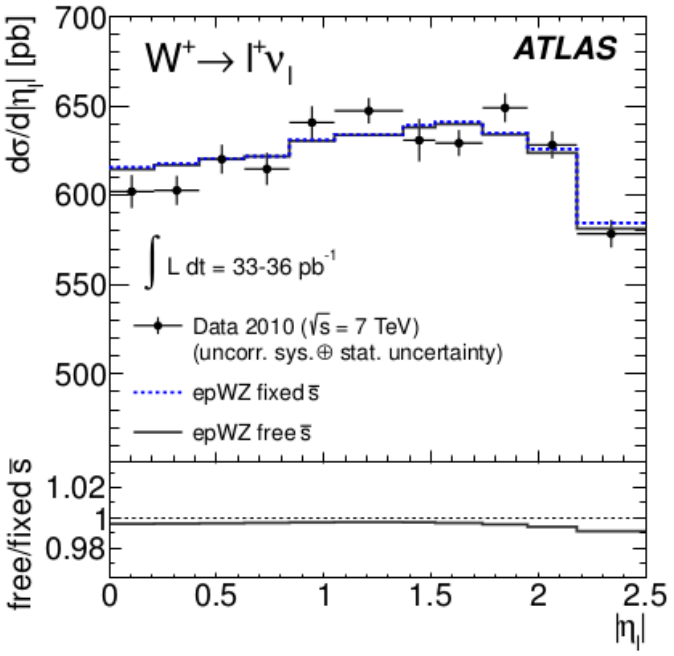

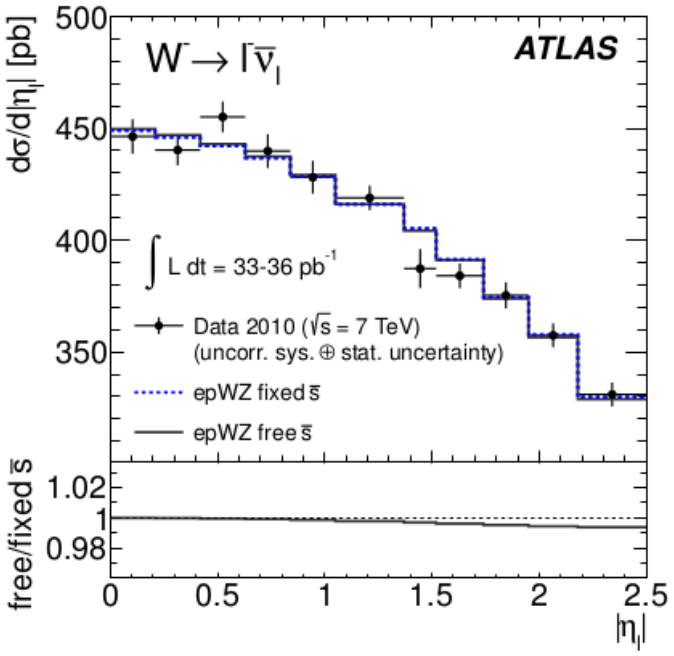

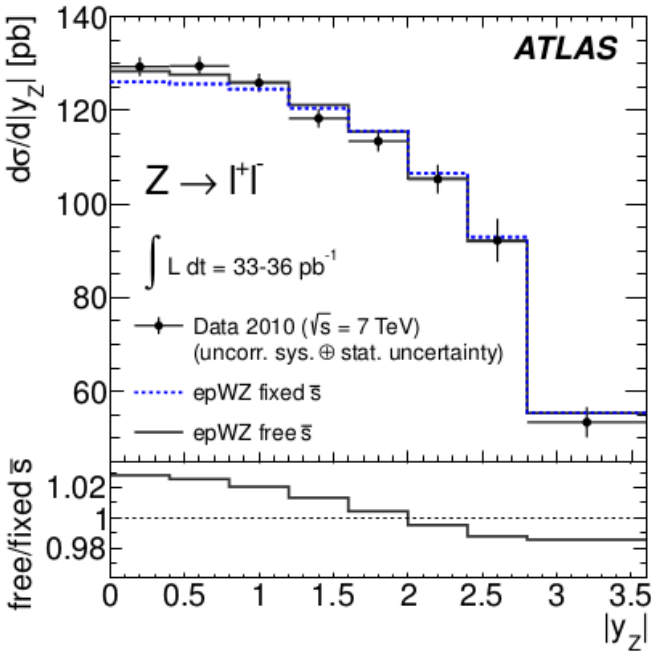

W± and Z cross section measurements are compared to epWZ with free and fixed strangeness. Also shown are the ratios of the epWZ fits. The enhanced strange quark fraction in the free s fit leads to an improvement in the description of the y_z distribution.

Strange quark density, strange-to-down sea quark distributions ratio

Constraining the PDF

1) Inclusive W/Z cross-sections

35 pb^{-1} of 7 TeV data (2010)

Phys.Rev.Lett. 109 (2012) 012001
– Phys. Rev. D85, 072004 (2012)

- $\sigma(W^+ + W^-)/\sigma(Z)$ is sensitive to the flavor composition of the quark sea

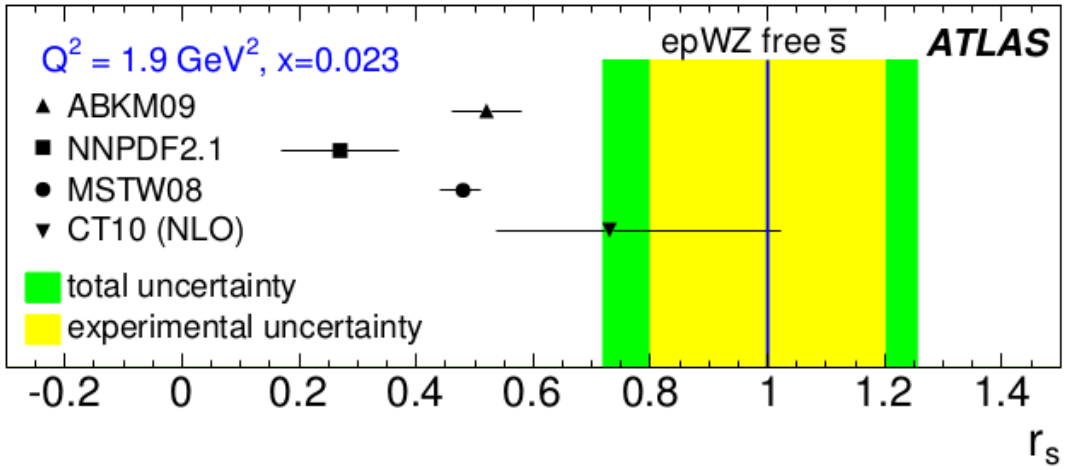

$$r_s = 0.5\left(s+\bar{s}\right)/\bar{d}$$

At Q_0^2 and x = 0.023, $r_s = 1.00\,^{+0.25}_{-0.28}$

For central rapidity Z data, x = 0.013 at $Q^2 = M_Z^2$, where $r_s(0.013, M_Z) = 1.00\,^{+0.09}_{-0.10}$

- Uncertainties are smaller at $Q^2 = M_Z^2$ because the g splitting probability into $q\bar{q}$ pairs is flavor independent, thus reducing any initial flavor asymmetries.

Valence quark density at low-x

Constraining the PDF

2) W/Z cross-section at 13 TeV

ATLAS-CONF-2015-039

- 85 pb^{-1}, 13 TeV

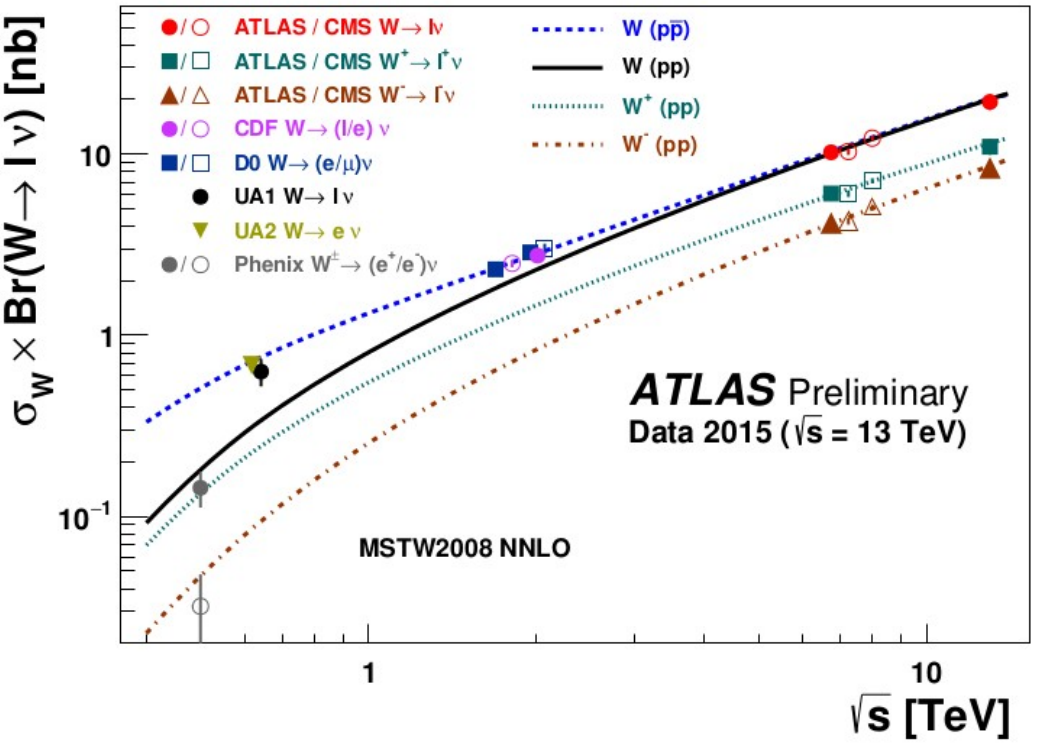

Measured total $W^{\pm}$ cross-sections, compared to theory predictions in pp, ppbar collisions in the combined electron-muon channel. The energy dependence of the cross-sections is well described.

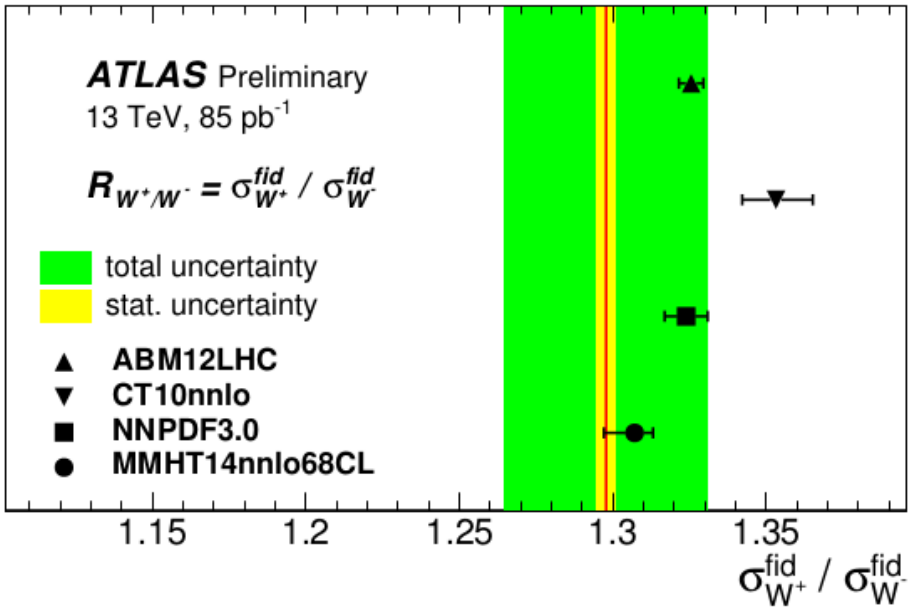

R(W+/W-) is sensitive to u_V and d_V at low-x. Significant scatter for different PDF sets, the favored ones are ABM12, NNPDF3.0 and MMHT14 which include data from LHC Run I.
Further constraints with more data.

Sensitive to parton flavor, probes the photon content of the proton

Constraining the PDF

3) Low Mass Drell-Yan $Z/\gamma^* \to \ell\ell\ (\ell = e, \mu)$ JHEP 06 (2014) 112

At low mass, the cross-section is dominated by electromagnetic couplings of $q\bar{q}$ to the virtual photon → different sensitivity to up- and down-type quarks compared to measurements near the Z resonance.

$26 < m_{ll} < 116$ GeV

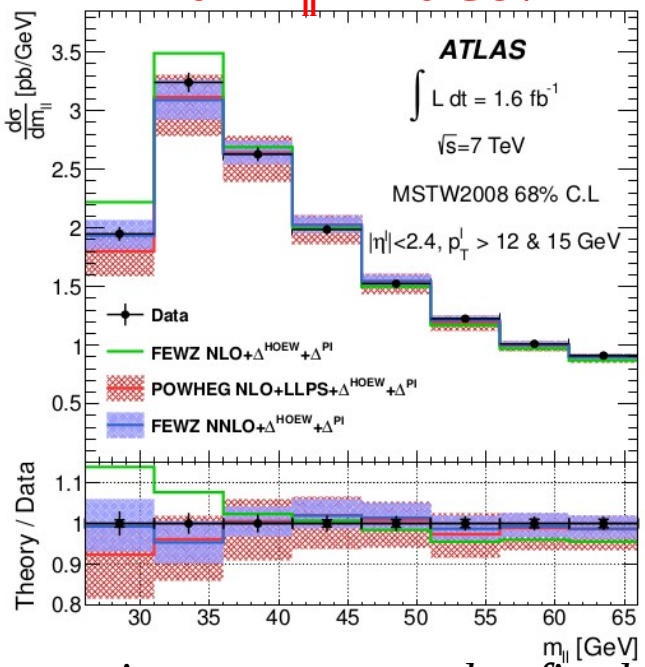

$12 < m_{ll} < 116$ GeV

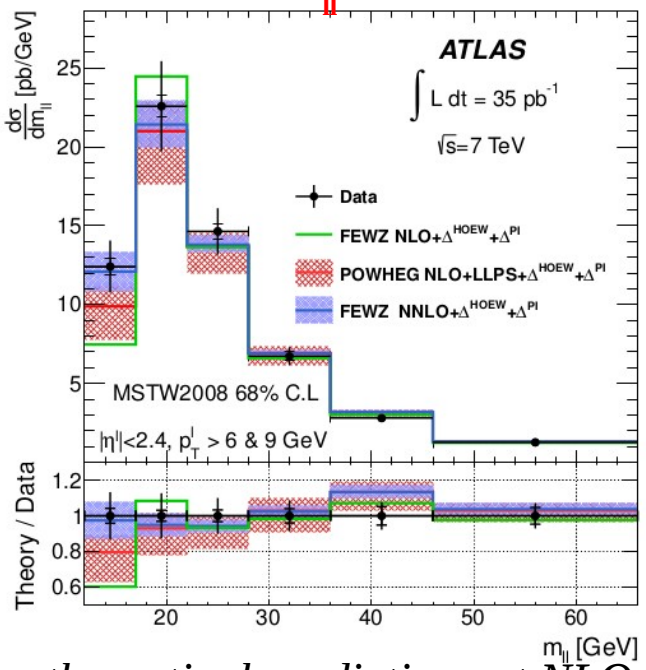

The fiducial cross sections are compared to fixed order theoretical predictions at NLO and NNLO from FEWZ, as well as an NLO+LLPS from Powheg.

- Prediction combining NNLO QCD + NLO EW provides significantly better fit to data than the pure NLO prediction.
- At this point the measurement is not precise enough to provide additional constraints on the PDFs.

Probes quark density functions at large-x

Constraining the PDF

4) High Mass Drell-Yan $Z/\gamma^* \to e^+e^-$

Phys. Lett. B 725 (2013) 223-242

- 4.9 fb^{-1} recorded in 2011 at 7 TeV
- $116 < m_{ee} < 1500$ GeV, $p_T > 25$ GeV
- This data can constrain the PDFs, particularly for quarks at large *x*
- *Figure : Measured differential cross-sections at Born level (before FSR), compared to FEWZ 3.1 calculations at NNLO QCD with NLO electroweak corrections*
- Predictions for all PDFs are consistent with the measured differential cross-section

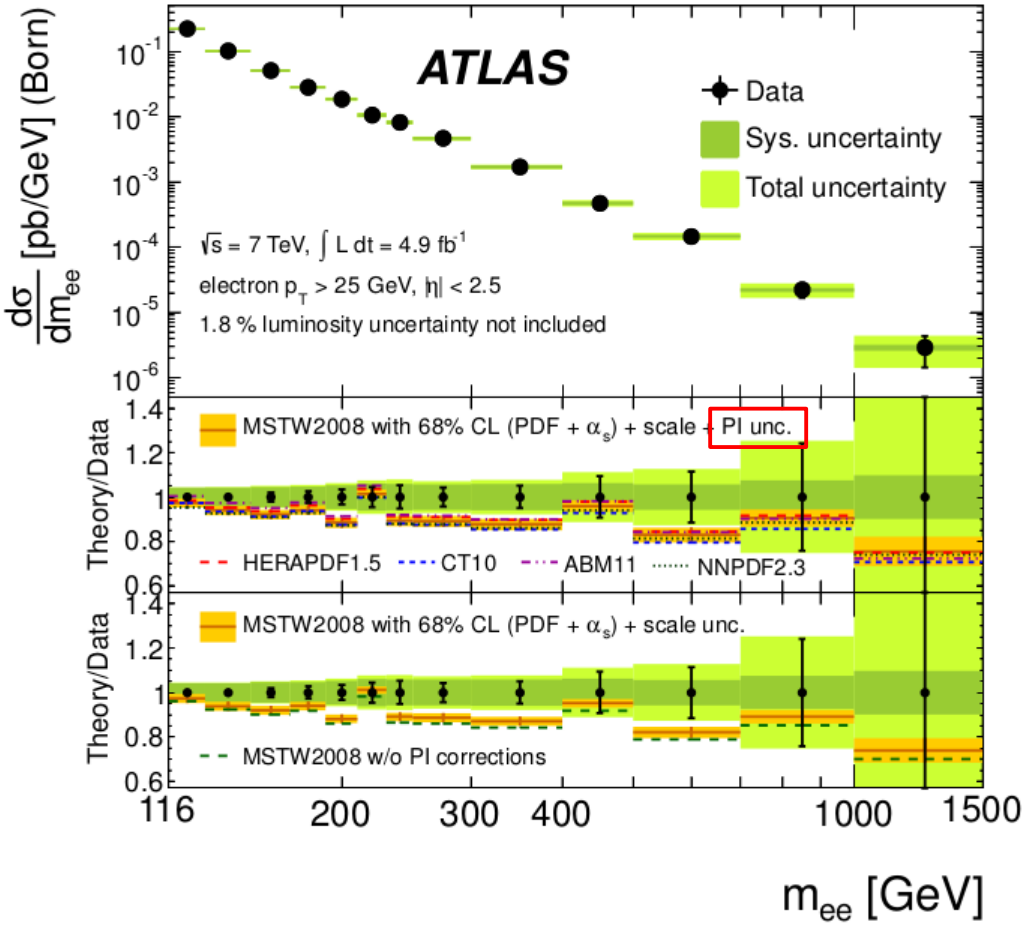

Directly sensitive to strange PDF

Constraining the PDF

5) W+c production

JHEP05(2014)068

Using 4.6 fb^{-1} of 7 TeV data (2011)

- Charm quark is tagged ⟨ μ from semileptonic charm decay within a hadronic jet
  charged D $^{(*)}$ (D or D *) meson
- The W and c are produced with opposite signs. The signal yield is defined as the difference between OS and SS events.

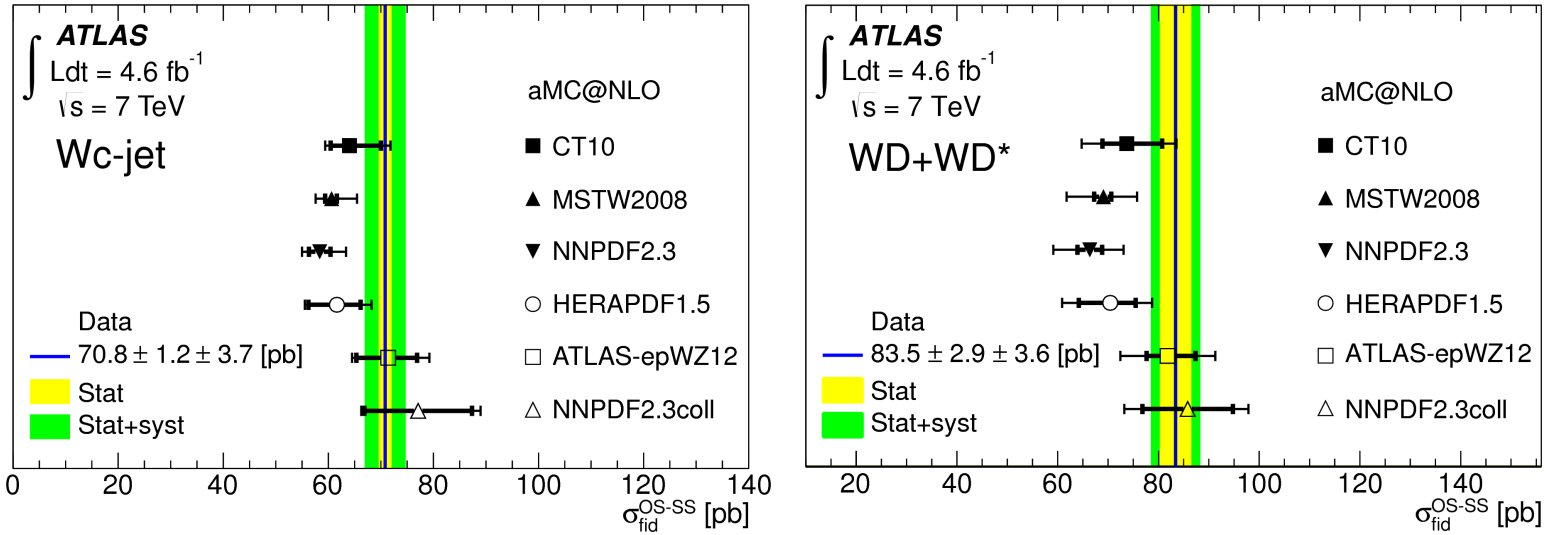

Measured fiducial cross sections compared to various PDF predictions based on aMC@NLO

All sets are consistent, but NNPDF2.3coll and ATLAS-epWZ12 sets are favored (these sets have non-suppressed strange). NNPDF2.3 is less favored.

Directly sensitive to strange PDF

Constraining the PDF

5) W+c production

JHEP05(2014)068

Using 4.6 fb^{-1} of 7 TeV data (2011)

- Charm quark is tagged ⟷ μ from semileptonic charm decay within a hadronic jet
  ⟷ charged D $^{(*)}$ (D or D *) meson
- The W and c are produced with opposite signs. The signal yield is defined as the difference between OS and SS events.

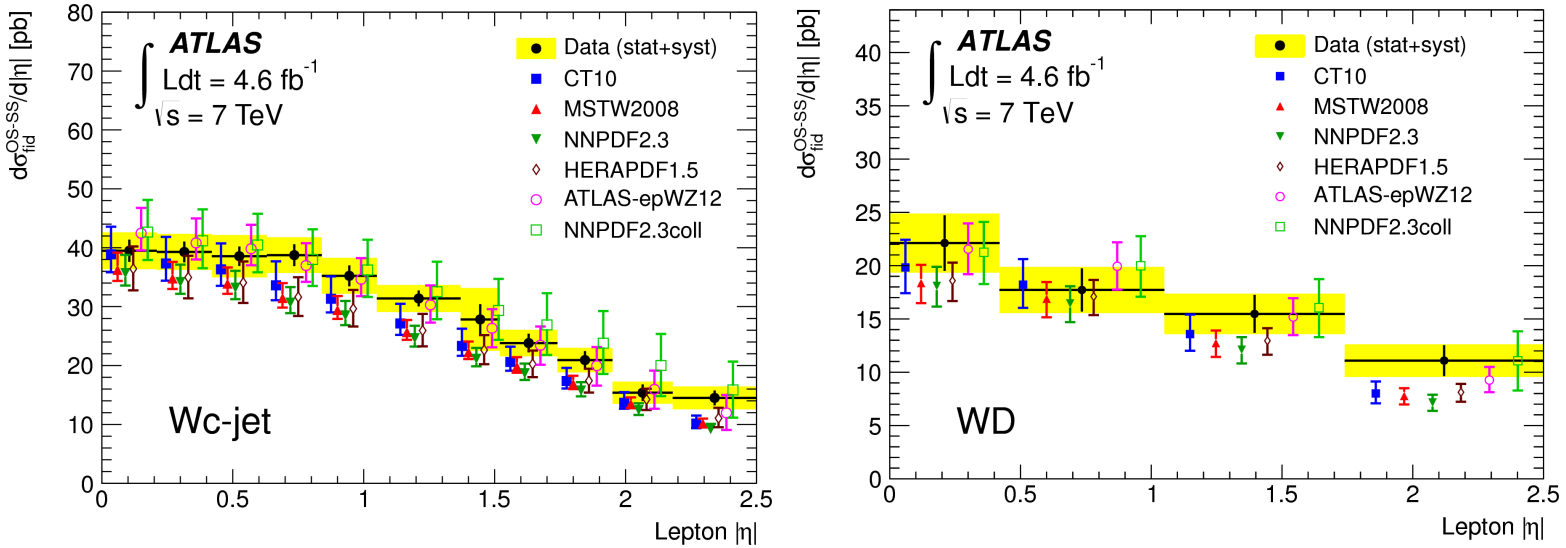

Measured differential cross section as a function of lepton |η| compared to predictions obtained using various PDF sets.

All sets are consistent, but NNPDF2.3coll and ATLAS-epWZ12 sets are favored (these sets have non-suppressed strange). NNPDF2.3 is less favored.

Directly sensitive to strange PDF

Constraining the PDF

5) W+c production

JHEP05(2014)068

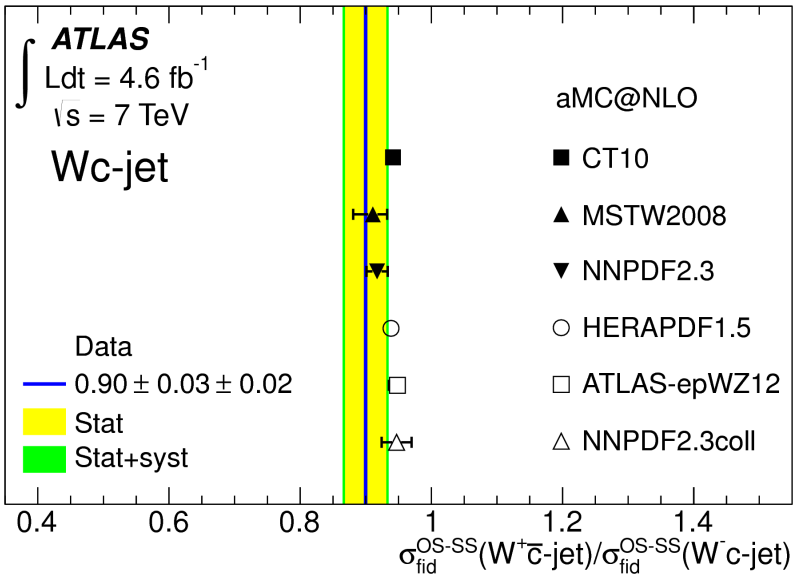

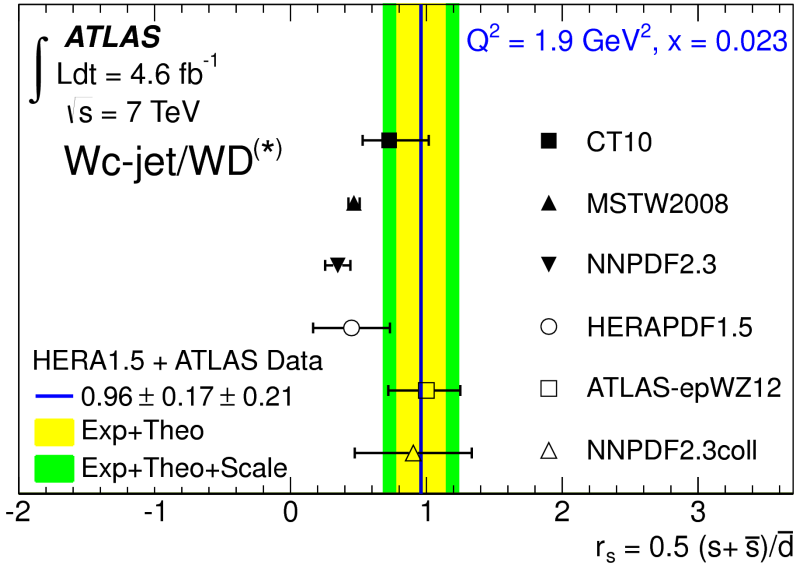

Measured ratios $\sigma(W^+ + \bar{c})/\sigma(W^- + c)$ *compared to various PDF predictions based on aMC@NLO.*
Consistent with all PDF sets within 1σ.

Strange-to-down ratio, at x = 0.023 and $Q^2 = 1.9\ GeV^2$ *:*

$$r_s = 0.96 \pm 0.17 \pm 0.21$$

In agreement with the r_s *determination in the W/Z cross-section measurement (previously discussed) :*

$$r_s = 1.00\ ^{+0.25}_{-0.28}$$

And supports the hypothesis of an SU(3)-symmetric light quark sea.

Sensitive to the gluon PDF

Constraining the PDF

6) Incl. jet, di-jet and 3-jet cross-sections JHEP 02 (2015) 153 - JHEP05(2014)059 - Eur. Phys. J. C (2015) 75

4.5 fb^{-1} of 7 TeV data

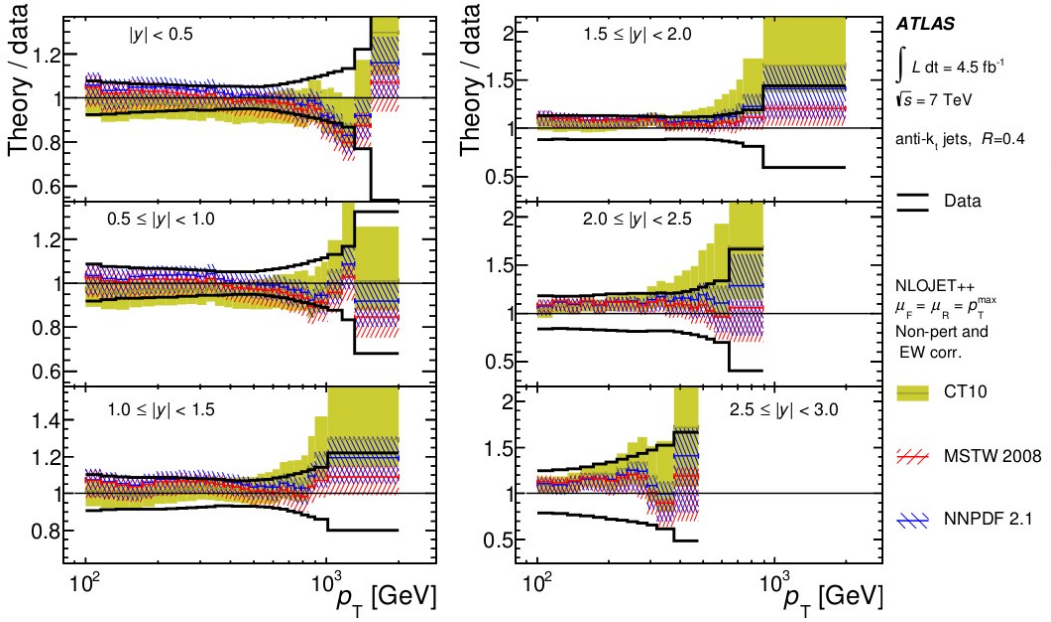

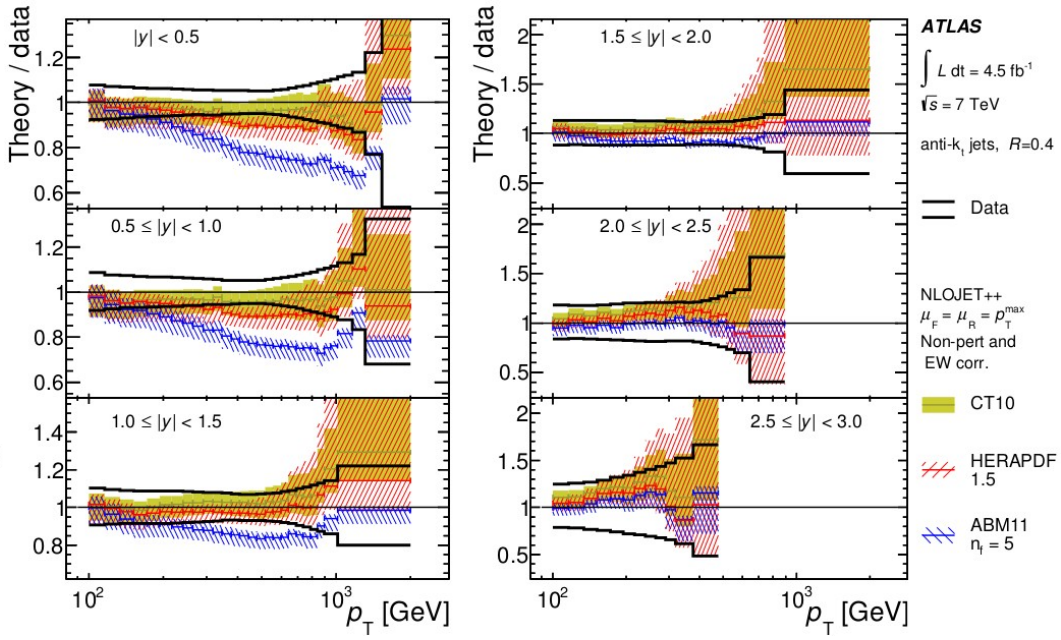

- **Inclusive jet cross section** : the predictions CT10, MSTW2008, NNPDF 2.1 (left), HERA1.5, ABM11 (right) are generally consistent with the measured cross-sections, except in a few bins (HERA, ABM at low rapidity).

Sensitive to the gluon PDF

Constraining the PDF

6) Incl. jet, di-jet and 3-jet cross-sections JHEP 02 (2015) 153 - JHEP05(2014)059 - Eur. Phys. J. C (2015) 75

4.5 fb^{-1} of 7 TeV data

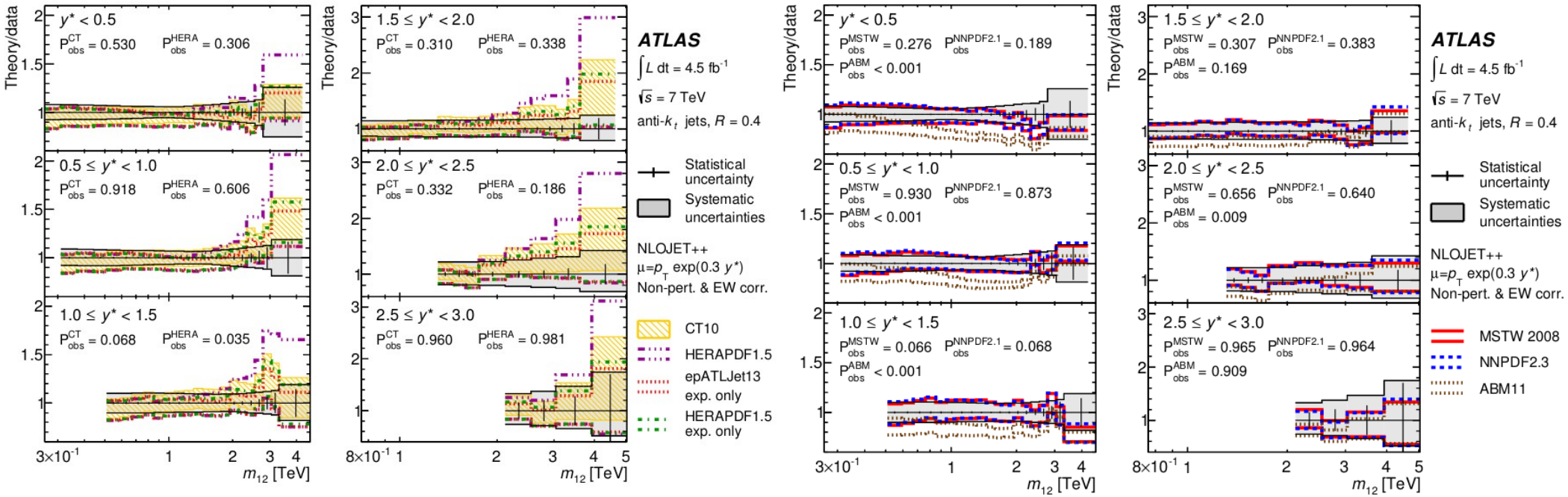

- **Di-jet cross section** : sensitivity to proton PDF is reduced at large y* because it is dominated by experimental uncertainties
- Agreement with CT10, NNPDF2.1, MSTW2008, disagreement in some bins with HERAPDF and a strong disagreement with ABM11.

Sensitive to the gluon PDF

Constraining the PDF

6) Incl. jet, di-jet and 3-jet cross-sections JHEP 02 (2015) 153 - JHEP05(2014)059 - Eur. Phys. J. C (2015) 75

4.5 fb^{-1} of 7 TeV data

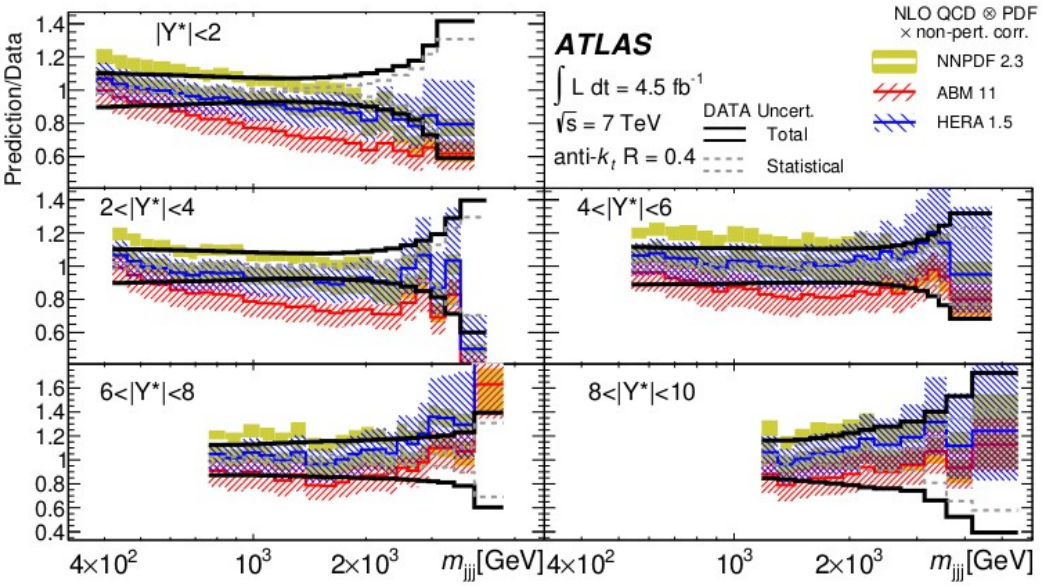

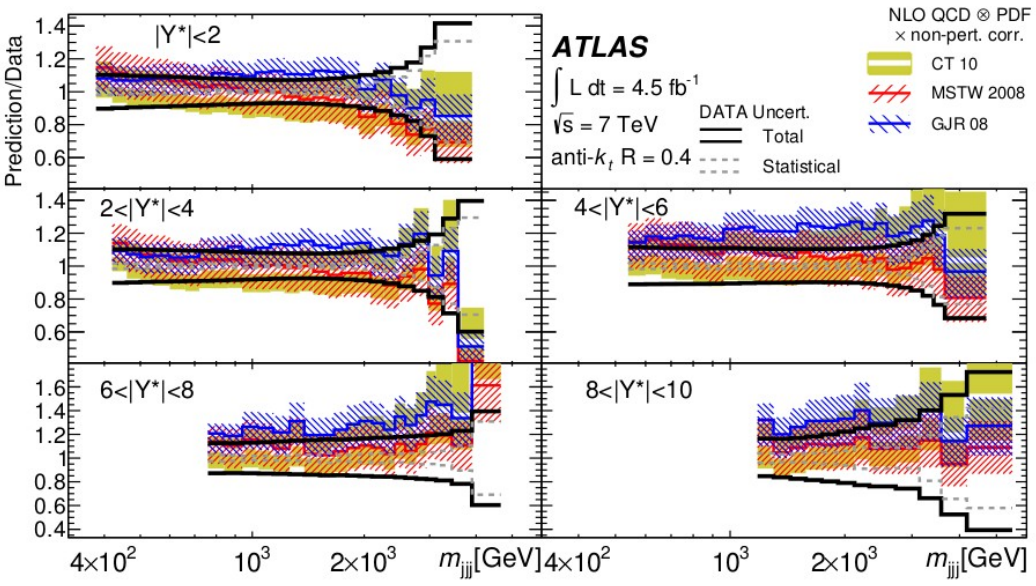

- **Three-jet cross section** : this measurement constrains the proton's PDFs in a different (x, Q^2) region than the inclusive and di-jet cross-sections.
- Good agreement with CT10, NNPDF2.3, GJR08, MSTW2008 and HERAPDF1.5, disagreement with ABM11

Sensitive to the gluon PDF

Constraining the PDF

7) Incl. jet cross-section at 2.76 TeV and 7 TeV

EPJC (2013) 73 2509

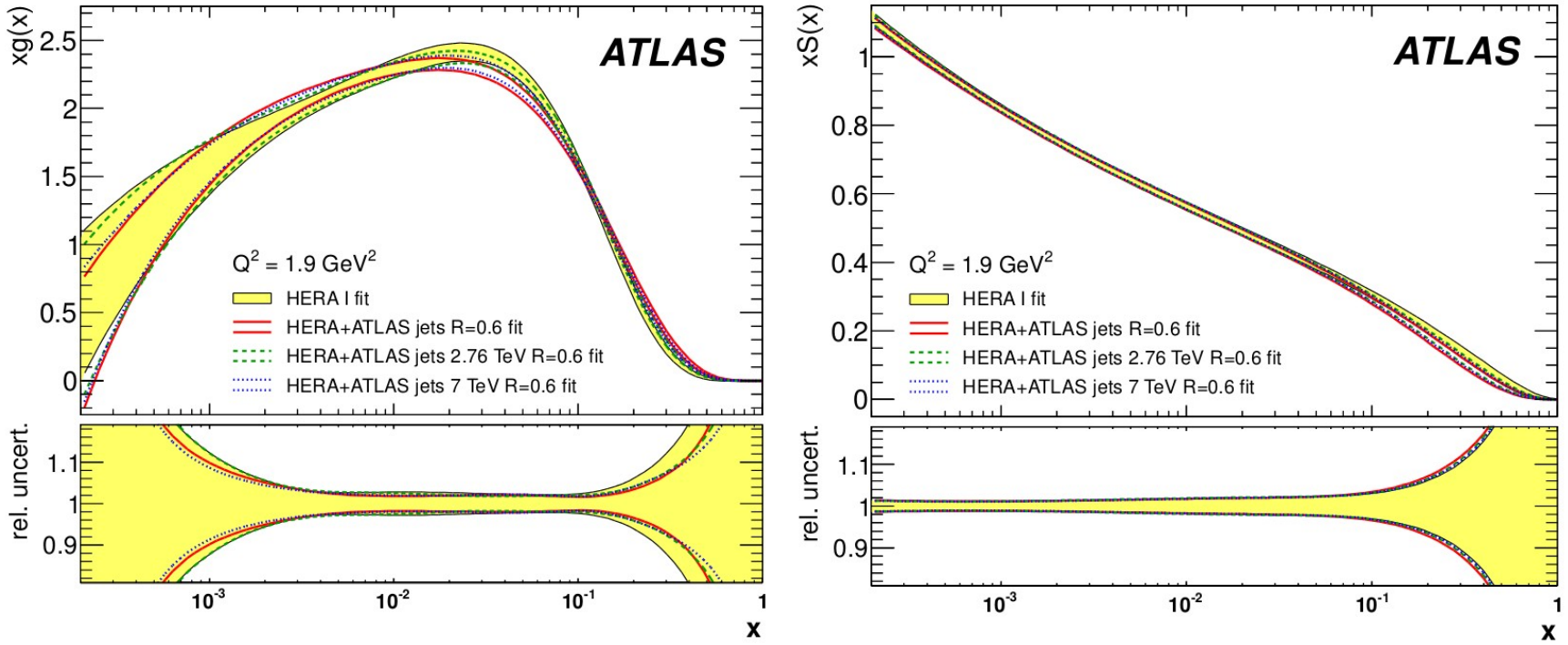

Momentum distributions of the gluon xg(s) and the sea quarks xS(x) using fits to HERA data alone and to HERA+ATLAS jet data

- Including ATLAS jet data → harder gluon distributions and softer sea quark distributions at high-*x*.
- ATLAS-epJet13 : new PDF set derived by including ATLAS data in HERA 1.5

Sensitive to gluon PDF

Constraining the PDF

8) Incl. isolated prompt γ cross-section

Phys. Rev. D 89, 052004 (2014)
ATL-PHYS-PUB-2013-018

- 4.6 fb^{-1} at 7 TeV

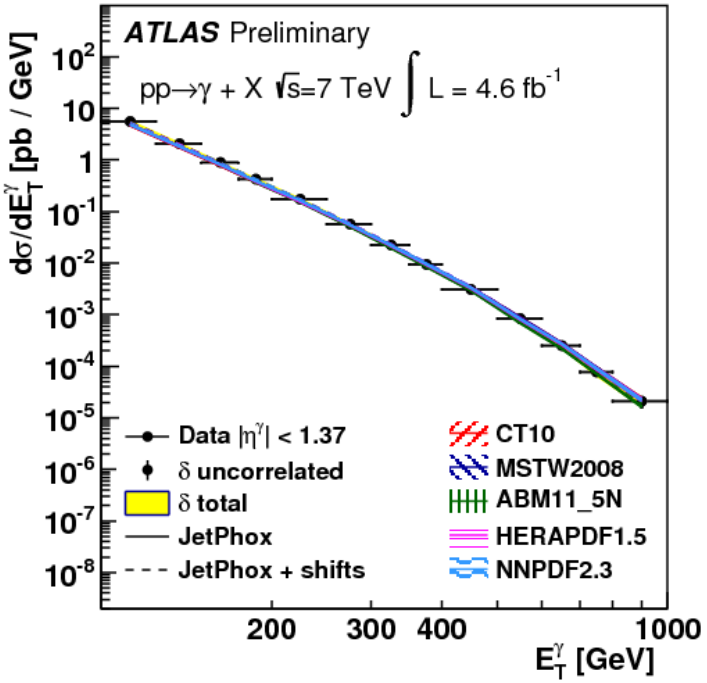

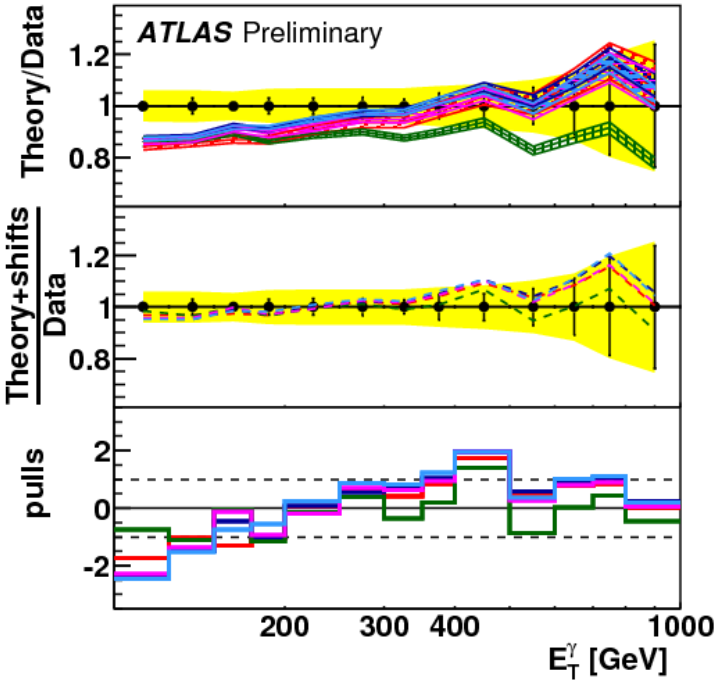

- Tension between the measured data and the predictions for many of the current PDF sets, reduced when including the PDF uncertainties.
- In the intermediate E_T region where the data are most precise, the scale uncertainty is dominant, thus NNLO calculations may be necessary to fully exploit the constraining potential of this measurement.

Sensitive to the gluon PDF

Constraining the PDF

9) Top quark production

Phys. Rev. D 90, 072004 (2014)

4.6 fb^{-1} , 7 TeV

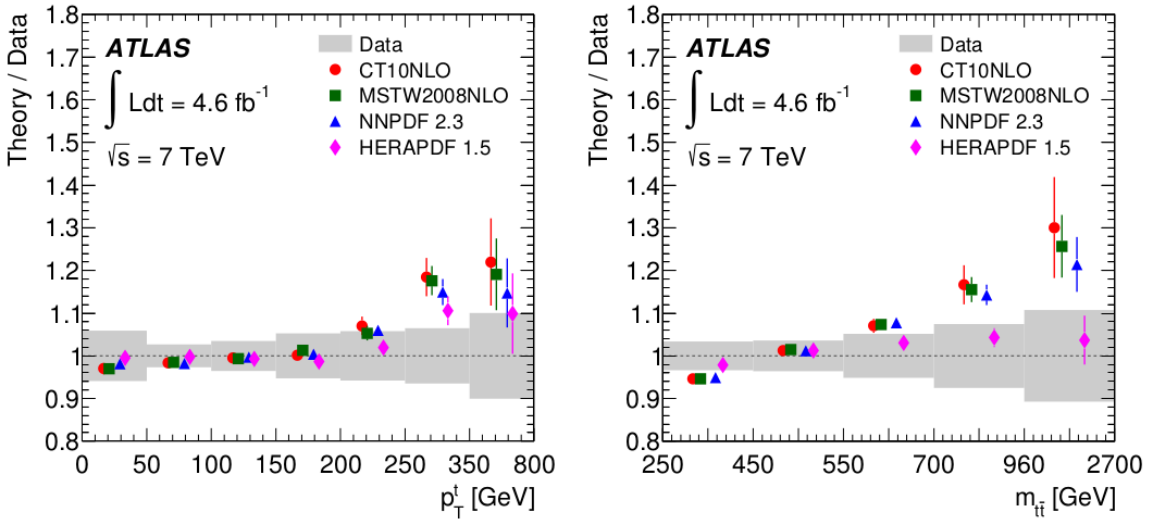

- Tension with all predictions at high p_T. For m_{tt}, agreement with HERAPDF1.5 (+NLO QCD calculations).
- Needed NNLO+NNLL calculations in QCD and after including electroweak effects.

10)Z-boson transverse momentum

- Sensitive to gluon PDF, but needs higher order QCD and EW corrections.
- Possible use of Z-p_T to constrain gluon PDF now that we have NNLO Z+1jet calculation.
- Complementary to other processes such as the direct photon production, the top-quark pair production and the jet production.

Summary

- Many measurements are affected by PDF uncertainties : Higgs production, electroweak measurement, heavy particles discoveries,... A better description of PDFs results in more precise measurements.
- The LHC energies allow for sensitive tests of perturbative QCD, and determination of the partonic content of the proton.
- PDF fits performed in ATLAS using W/Z, W+c and jet data, lead to improving the knowledge on the strange and gluon densities.
- Further constraints are expected from the coming measurements at 13 TeV.

Back-up slides

W-boson mass (PDF uncertainties)

ATL-PHYS-PUB-2014-015

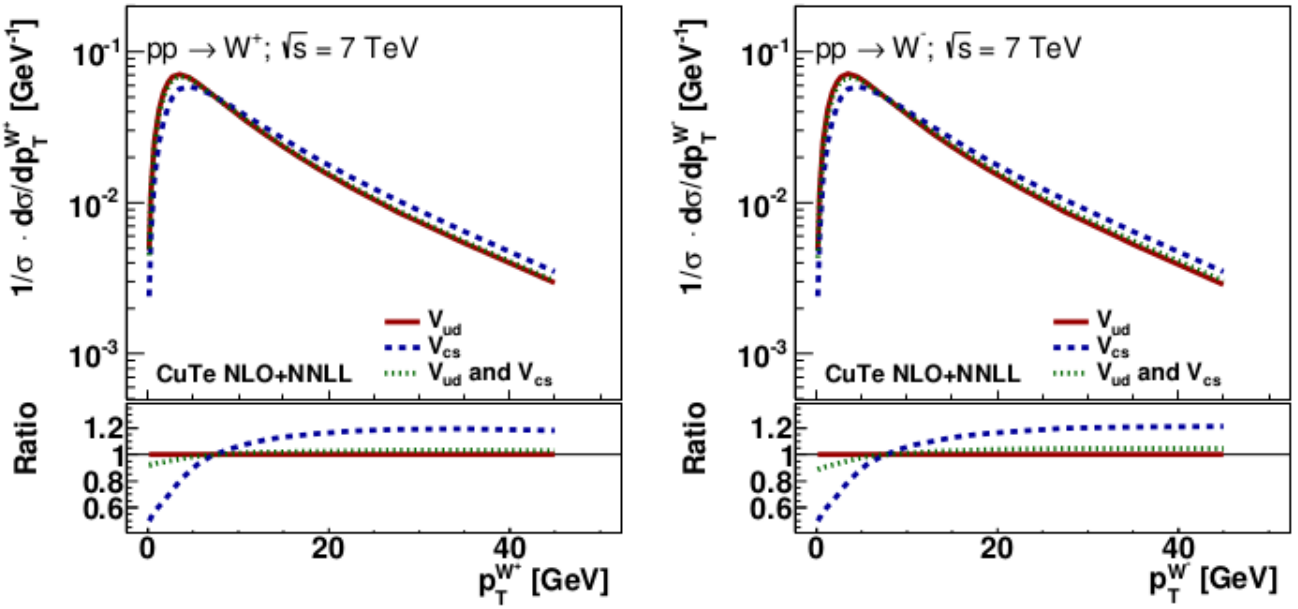

Normalised differential cross sections as a function of p_T^W for W^+ and W^- production. The spectra corresponding to only V_{ud}, only V_{cs}, and only V_{ud} and V_{cs} CKM matrix elements are compared.

	MW-NLO	CT10nlo	MSTW2008CPdeutnlo	NNPDF30_nlo_as_118
W^+	+13 -12	+18 -22	+11 -10	+8 -10
W^-	+22 -22	+18 -23	+11 -10	+8 -9
$W^\pm$	+11 -11	+14 -18	+7 -7	+6 -5

Summary of PDF uncertainties (MeV) for the extraction of m_W from the p_T spectrum.

W-boson mass (PDF uncertainties)

ATL-PHYS-PUB-2014-015

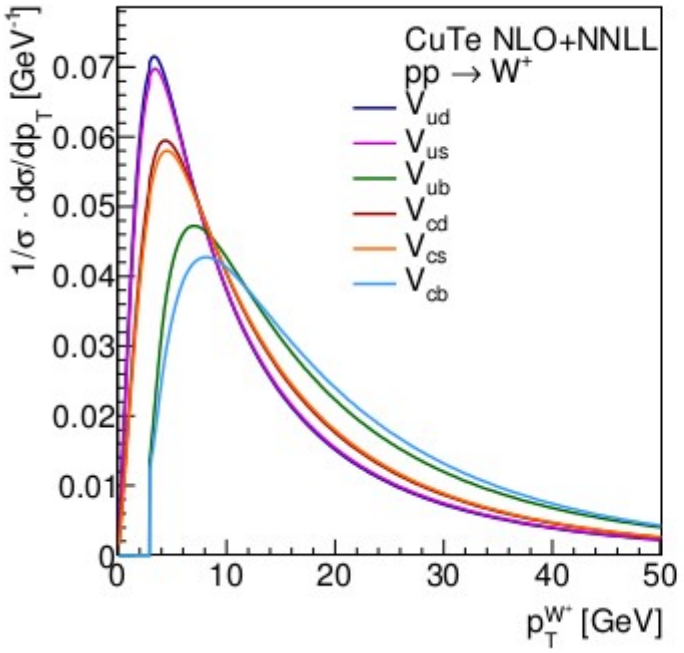

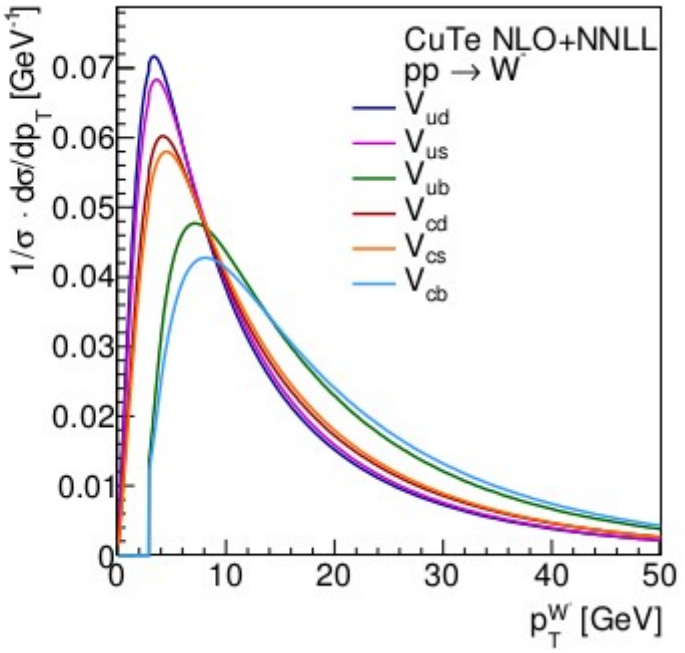

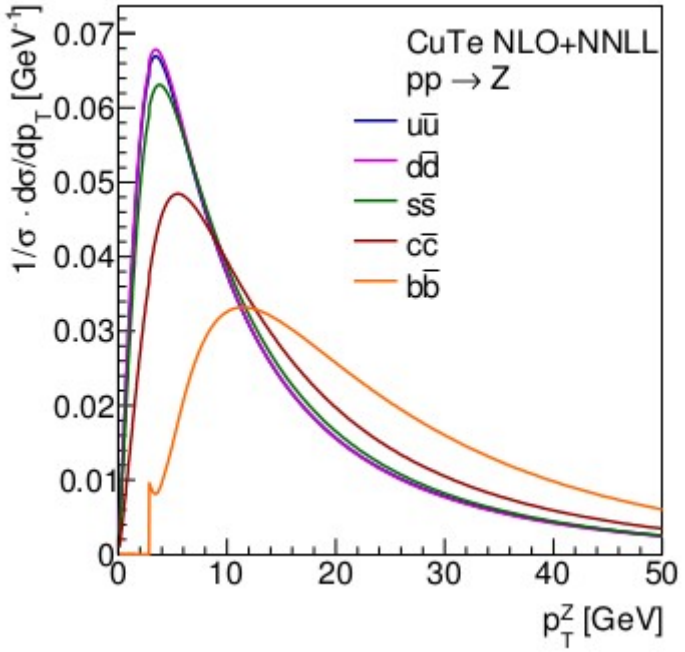

Differential cross sections as a function of $p_T^{W,Z}$ for W^+, W^- and Z production for different initial parton flavors, as evaluated by CuTe at NLO+NNLL. All distributions are normalized to the same area.

W/Z cross-section at 13 TeV

ATLAS-CONF-2015-039

- 85 pb^{-1}, 13 TeV

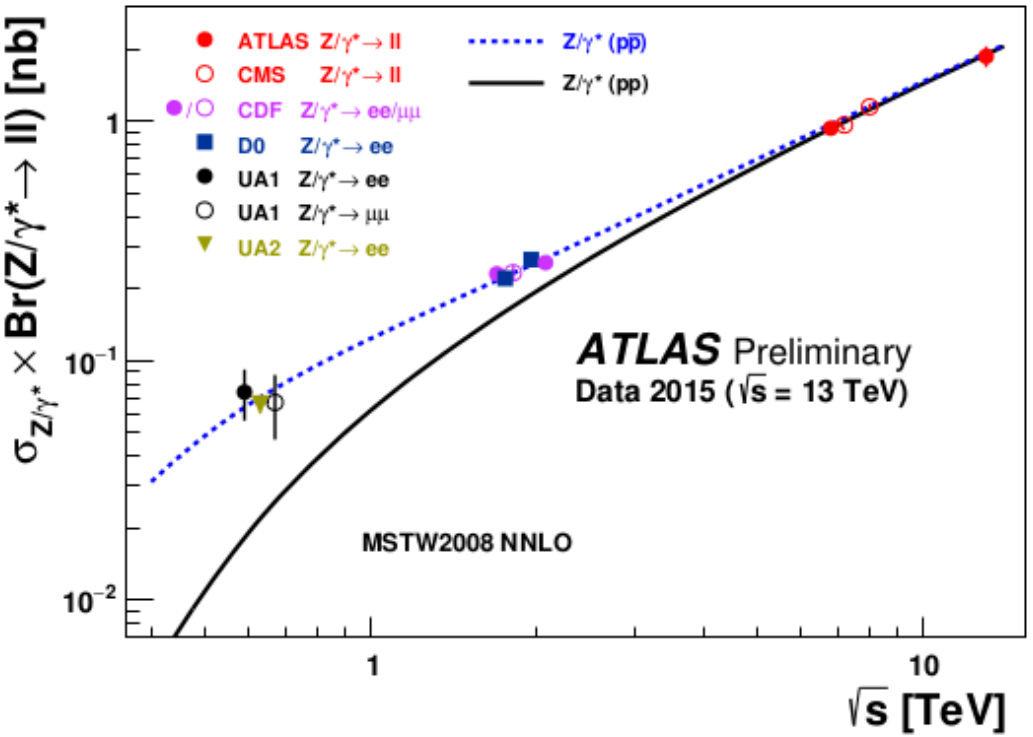

Measured total Z cross-sections, compared to theory predictions in pp, ppbar collisions in the combined electron-muon channel. The energy dependence of the cross-sections is well described.

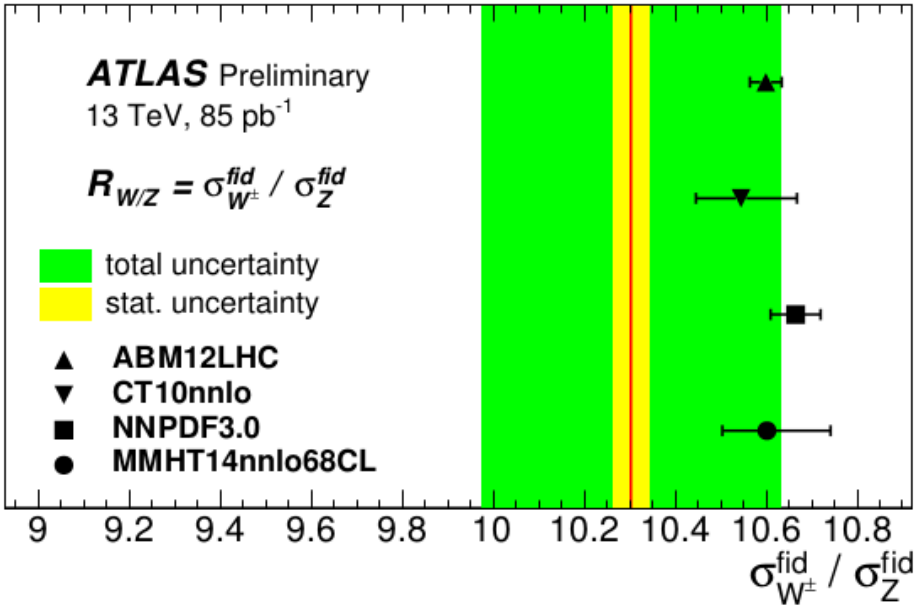

R(W±/Z) constrains s-quark distributions
Measurement consistent with all PDF sets

Low Mass Drell-Yan $Z/\gamma^* \to \ell\ell\ (\ell = e, \mu)$ JHEP 06 (2014) 112

Nominal Measurement	$26 < m_{ll} < 66$ GeV	$p_T^l > 12\&15$ GeV	2011, 7 TeV data (1.6 fb^{-1})
Extended Measurement (μ channel only)	$12 < m_{ll} < 66$ GeV	$p_T^l > 6\&9$ GeV	+ 2010, 7 TeV data (35 pb^{-1})

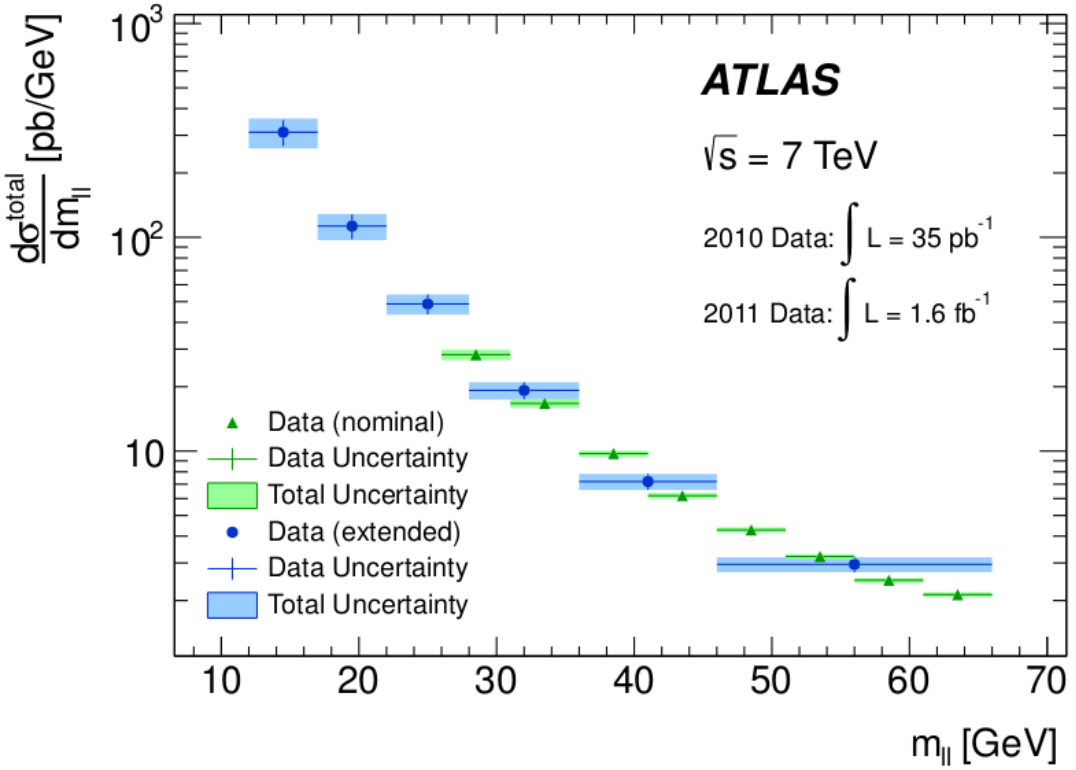

Comparison of Born-level nominal (e + μ) and extended (μ) channel differential cross sections as a function of the dilepton invariant mass, m_{ll}, extrapolated to full phase space.

Inclusive jet cross section

JHEP 02 (2015) 153

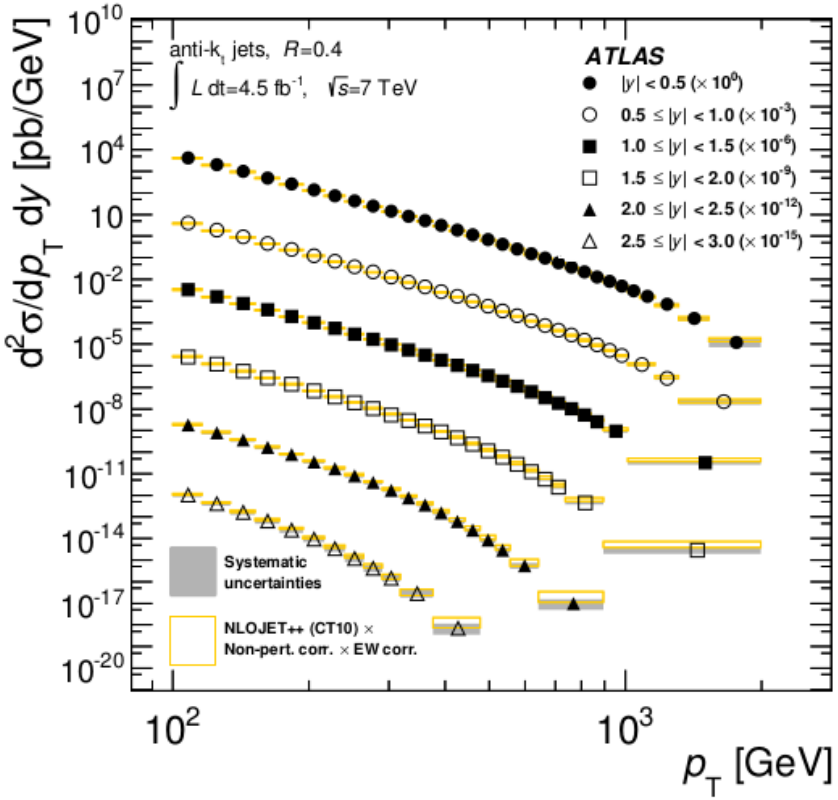

Double-differential inclusive jet cross-sections as a function of the jet p_T in bins of rapidity

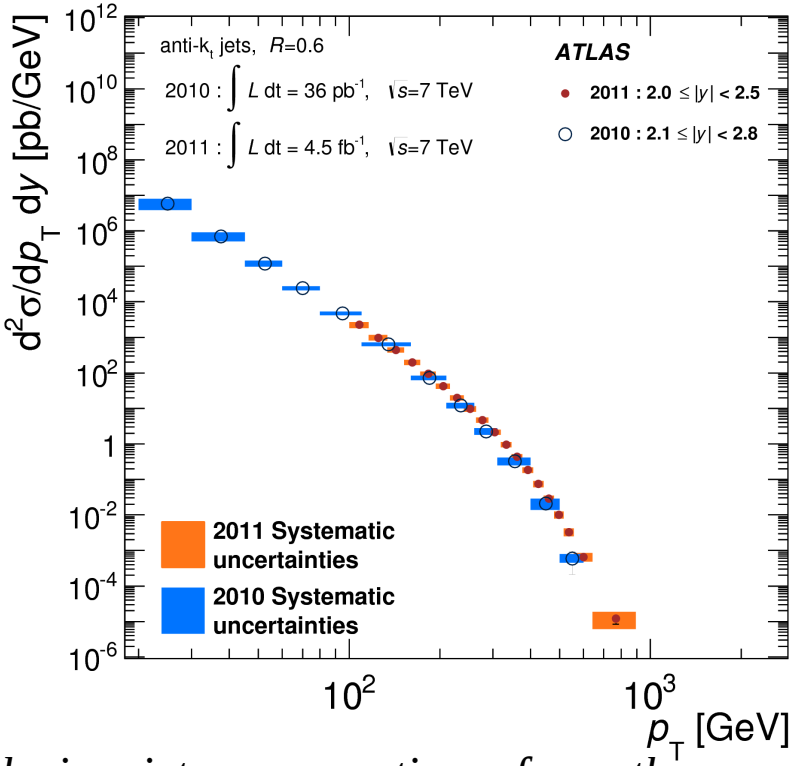

Inclusive jet cross-sections from the measurement using 2010 data and those using 2011 data, as a function of the jet p_T in the lowest rapidity bins, for anti-k_T jets with R=0.6.

The sizes of the rapidity bins differ between the two measurements, hence only a qualitative comparison is possible.

Di-jet cross section (left)

JHEP05(2014)059

4.5 fb^{-1}, 7 TeV, double differential cross-sections as a function of dijet mass and half the rapidity separation of the two highest-p_T jets $y^* = |y_1 - y_2|/2$

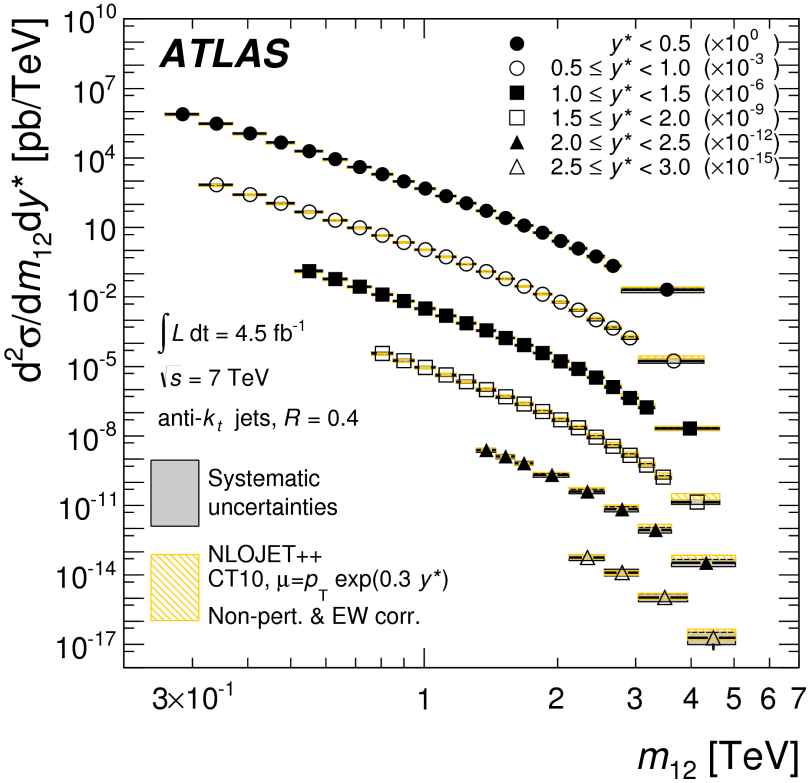

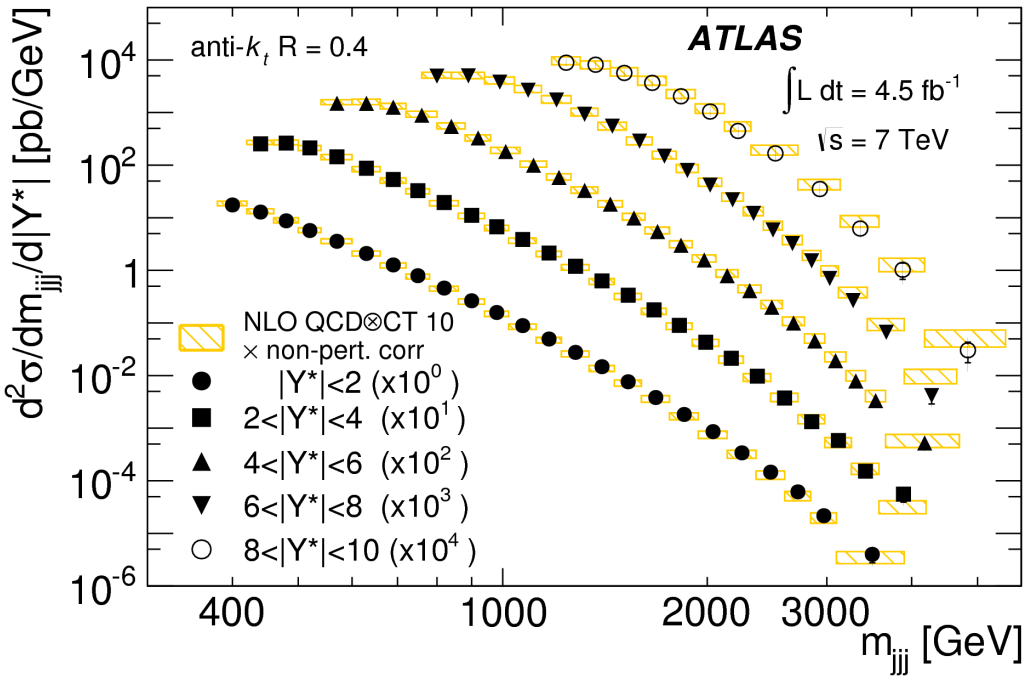

Three-jet cross section (right)

Eur. Phys. J. C (2015) 75

4.5 fb^{-1}, 7 TeV, double differential cross-sections as a function of 3-jet mass, $m_{jjj} = \sqrt{(p_1 + p_2 + p_3)^2}$ and the sum of absolute rapidity separation between the three leading jets, $|Y^*| = |y_1 - y_2| + |y_2 - y_3| + |y_1 - y_3|$

Incl. jet, di-jet cross-sections

JHEP 02 (2015) 153 - JHEP05(2014)059

y ranges	R = 0.4 NLO PDF set:	P_{obs} CT10	MSTW2008	NNPDF2.1	HERAPDF1.5	ABM11
$\|y\| < 0.5$		84%	61%	72%	56%	<0.1%
$0.5 \le \|y\| < 1.0$		91%	93%	89%	49%	<0.1%
$1.0 \le \|y\| < 1.5$		89%	88%	85%	93%	2.7%
$1.5 \le \|y\| < 2.0$		93%	88%	91%	75%	55%
$2.0 \le \|y\| < 2.5$		86%	82%	85%	26%	57%
$2.5 \le \|y\| < 3.0$		95%	94%	97%	82%	85%

y ranges	R = 0.6 NLO PDF set:	P_{obs} CT10	MSTW2008	NNPDF2.1	HERAPDF1.5	ABM11
$\|y\| < 0.5$		52%	45%	57%	17%	<0.1%
$0.5 \le \|y\| < 1.0$		31%	47%	40%	3.8%	<0.1%
$1.0 \le \|y\| < 1.5$		95%	92%	90%	92%	2.3%
$1.5 \le \|y\| < 2.0$		89%	85%	86%	94%	58%
$2.0 \le \|y\| < 2.5$		84%	88%	89%	49%	72%
$2.5 \le \|y\| < 3.0$		88%	98%	97%	76%	78%

PDF set	y^* ranges	mass range (full/high)	P_{obs} $R = 0.4$	$R = 0.6$
CT10	$y^* < 0.5$	high	0.742	0.785
	$y^* < 1.5$	high	0.080	0.066
	$y^* < 1.5$	full	0.324	0.168
HERAPDF1.5	$y^* < 0.5$	high	0.688	0.504
	$y^* < 1.5$	high	0.025	0.007
	$y^* < 1.5$	full	0.137	0.025
MSTW 2008	$y^* < 0.5$	high	0.328	0.533
	$y^* < 1.5$	high	0.167	0.183
	$y^* < 1.5$	full	0.470	0.352
NNPDF2.1	$y^* < 0.5$	high	0.405	0.568
	$y^* < 1.5$	high	0.151	0.125
	$y^* < 1.5$	full	0.431	0.242
ABM11	$y^* < 0.5$	high	0.024	$< 10^{-3}$
	$y^* < 1.5$	high	$< 10^{-3}$	$< 10^{-3}$
	$y^* < 1.5$	full	$< 10^{-3}$	$< 10^{-3}$

- Inclusive jet cross section (left) : the predictions (CT10, MSTW2008, NNPDF 2.1, HERA1.5, ABM11) are generally consistent with the measured cross-sections, exceptions : highlighted.
- Di-jet cross section (right) : agreement with CT10, NNPDF2.1, MSTW2008, disagreement in some bins with HERAPDF and a strong disagreement with ABM11.

Z-boson transverse momentum

JHEP09(2014)145

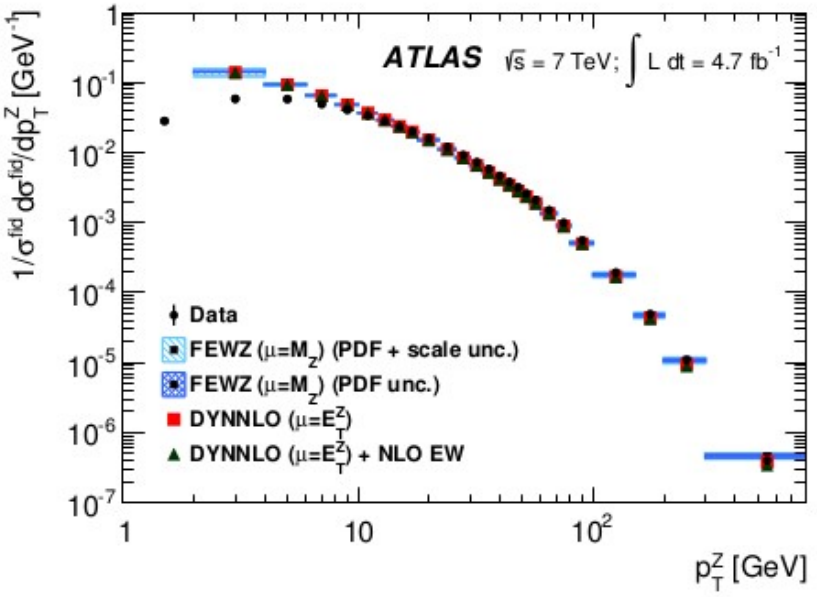

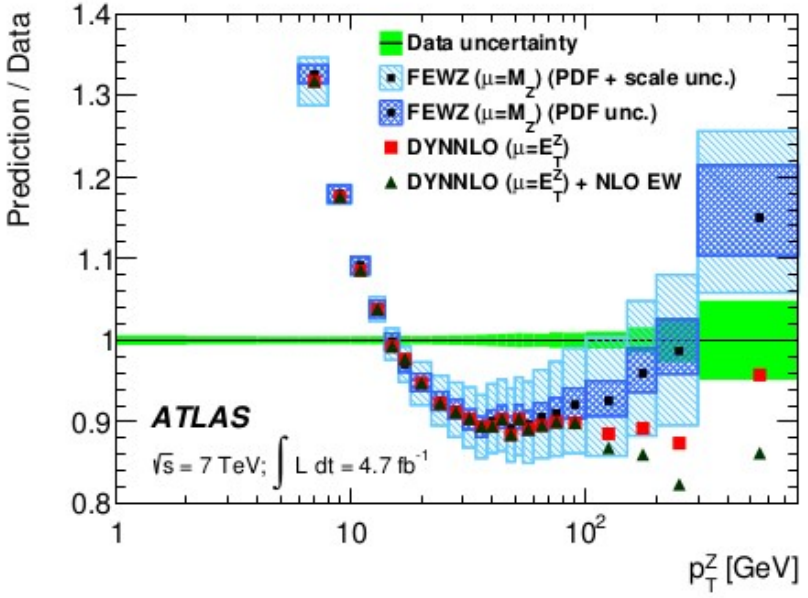

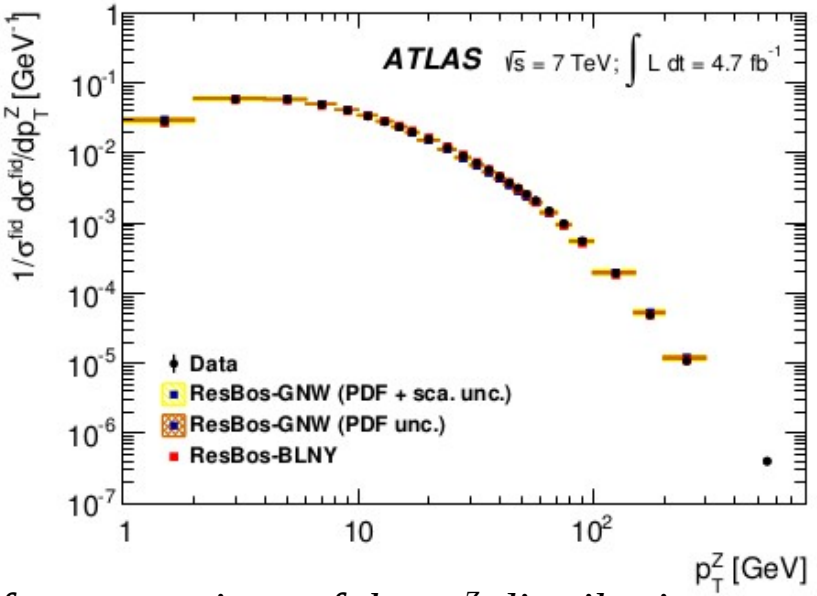

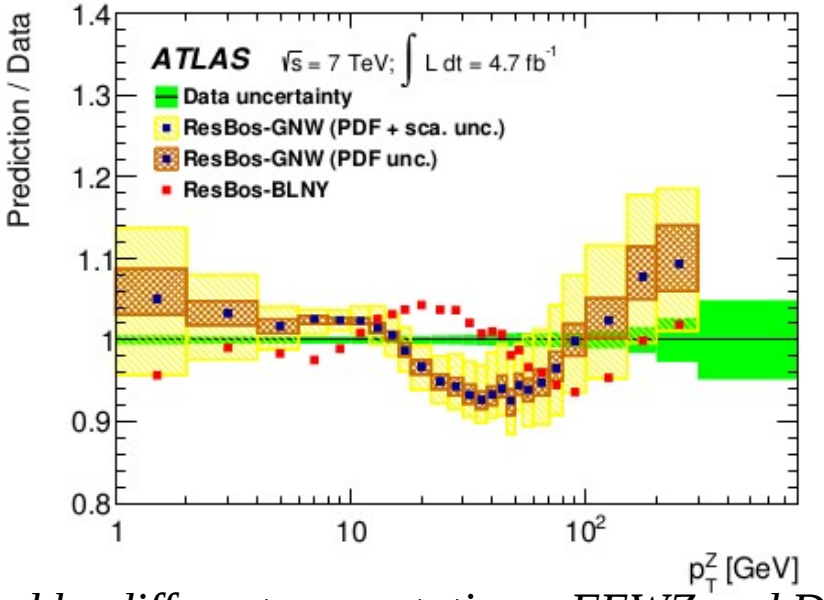

Left : comparison of the p_T^Z distributions predicted by different computations: FEWZ and DYNNLO (top) and ResBos (bottom) with the Born-level combined measurement, inclusively in y_Z.
Right : ratios between these predictions and the combined measurement.